Probing the dusty environment of Gamma-Ray bursts using late X-ray observations

PI: Arushi Kumar

1. Abstract

Long-duration gamma-ray bursts (GRBs) are associated with the collapse of massive stars and often occur in dusty surroundings. Scattering of prompt X-rays by dust near the burst site creates a delayed echo, visible during the afterglow phase and causes late-time spectral changes in the X-ray light curve. Models predict an initial softening when the dust-scattered flux dominates the external shock emission, followed by spectral hardening as the external shock emission reappears later, in timescales of a few tens of days. To capture the full evolution, deep late-time observations with XMM-Newton is necessary. We propose to use the XMM-Newton EPIC observations of one GRB to probe host dust properties and to understand the progenitors and environment of the burst.

2. Description of the proposed programme

A) Scientific Rationale:

A class of GRBs, mostly with prompt emission lasting a few seconds or more, is believed to originate from the collapse of massive stars. Most nearby bursts of this class are associated with hydrogen-deficient type Ib/c supernovae (Galama et al., 1998; Hjorth et al., 2003), indicating the progenitors to be massive Wolf-Rayet (WR) stars. Massive WR stars in our galaxy are found to be surrounded by dusty regions, such as dust shells (Tuthill et al., 1999; Paul, 2003). Consistent with this observation, the optical/UV afterglows of some GRBs are heavily extinguished, indicating the presence of strong line-of-sight absorption due to dust layers in the host galaxy (Holland et al., 2010). These are called "optically dark bursts." Observations of GRB host galaxies further support the presence of dust near GRB sites (Perley et al., 2013).

Multi-band modelling of afterglows allows us to infer the properties of the line-of-sight dust column in the host galaxy, such as grain size distribution and composition, based on the observed spectral shape within the IR/optical/UV bands. Several studies have found that the dust in GRB hosts differs from that in the Milky Way and more closely resembles that of star-forming galaxies (Schady et al., 2012).

In this proposal, to probe the dust around the GRB sites, we aim to study the X-ray photons scattered by dust layers. The X-ray photons emitted during the prompt phase of the GRB can scatter off dust layers near the progenitor. These reprocessed photons travel a longer distance and arrive later during the afterglow phase (Klose, 1998; Miralda-Escude, 1998; Meszaros et al., 2000; Shao & Dai, 2007). The scattered component has a power-law spectrum similar to the afterglow synchrotron or IC radiation, but with a much steeper index (i.e., softer spectrum) that depends on the prompt emission spectrum and the grain size distribution. Therefore, the delayed arrival of these photons results in a time evolution of the afterglow X-ray spectral index (Klose, 1998; Shao & Dai, 2007).

Studying the reprocessed X-ray emission allows us to infer the distance of the dust layer from the GRB source, the average density of the dust shell, and the grain size distribution which is parameterised by the minimum and maximum grain size ($a_{\rm min}$ and $a_{\rm max}$ respectively) and the power-law index q of the distribution.

A sample of GRBs are found to exhibit this spectral softening (Wang et al., 2016; Margutti et al., 2015). Examples that concentrate on explaining the spectral evolution of individual bursts using the dust echo model include GRB 130925A (Evans et al., 2014), GRB 060218A (Irwin et al. 2016), and our ongoing work on GRB 130907A ((Mandayapuram et al. in prep).

Our group started studying the spectral evolution of dusty GRBs to understand how the X-ray spectrum of GRB afterglows changes at late times. The X-ray data of around ten GRBs were analysed, and the light curve and spectral index were obtained self-consistently. It was found that GRB 130907A exhibited the most significant spectral variation among the entire sample.

B) Immediate Objective:

The optical depth to scattering depends on the photon energy E and the grain size (a). The scattered spectrum is a convolution of the incident spectrum and the energy-dependent optical depth. It evolves from $E^{-s-2}\mathcal{S}(E)$ at early times to $E^{-s+2}\mathcal{S}(E)$ late times, where $\mathcal{S}(E)$ is the prompt spectrum and s characterises the energy dependence of optical depth (Shao et al., 2007). The timescale of evolution for a given band depends on the distance R to the dust layer, and for typical values can be about a day.

However, since the afterglow phase contains both external shock emission and the reprocessed emission, the resulting spectral evolution is more complex and depends on the relative brightness of these two components.

In Figure 1, we show the light curve and spectral evolution for three different combinations of afterglow normalisation and dust properties (R and the parameters of grain size distribution). The spectral peak indicates when the contributions from the dust echo and external shock are equal; specifically, before this peak, the emission is primarily composed of soft, delayed, scattered prompt X-ray photons, whereas after the peak, the forward-shock synchrotron emission takes precedence, resulting in hardening.

It is evident that multiple possibilities can reproduce the data. For example, the orange curve corresponds to a fully dust emission-dominated afterglow, and the blue curve corresponds to a case where the early time is dominated by the external shock, following which the dust emission dominates, and even later the afterglow becomes prominent again. Hence, obtaining reliable parameter estimates requires long-term X-ray monitoring, particularly around ~ 10 days and beyond.

And this is precisely where XMM-Newton becomes crucial. By observing GRB afterglows at late epochs, we can track how the X-ray spectrum softens or hardens and identify the contribution of dust-scattered prompt emission.

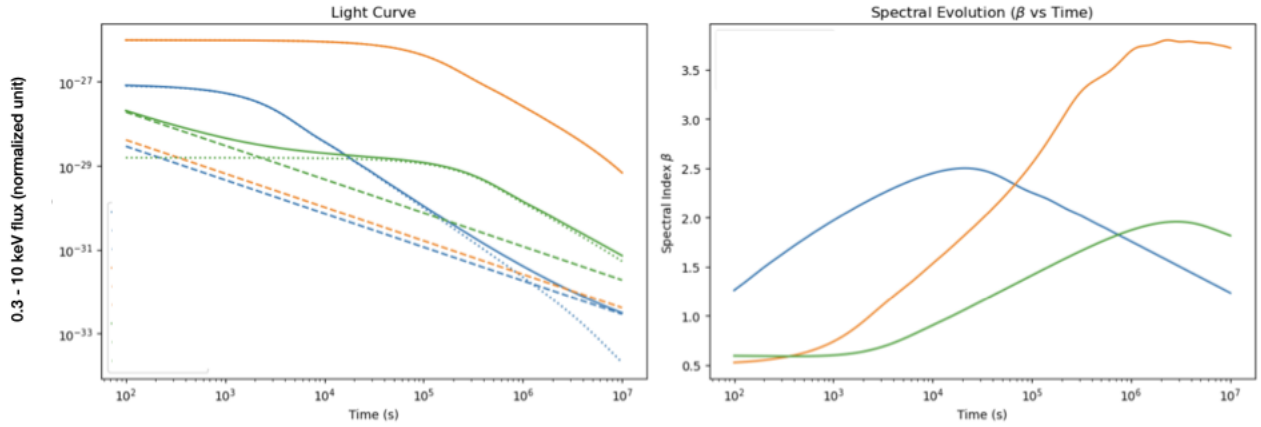

Figure 1: (Left) Simulated afterglow light curves with external shock and dust-scattered prompt emission component for three combinations of parameters. Total flux (solid), dust scattered emission (dotted), and external shock emission (dashed). (Right) Evolution of the afterglow spectral index (β) for the same parameters. The rise in β indicates softening of the spectrum, due to increasing dominance of the dust scattering component over the external shock emission, and the fall indicates the hardening due to reemergence of the external shock.

3. Justification of requested observing time, feasibility and visibility

Beyond a few days, Swift XRT count rates typically drop to $\leq 10^{-2}$ s^{-1}, making it difficult to constrain the spectral index. XMM-Newton's larger effective area enables detection and spectral characterisation of faint late-time emission, including dust-scattered X-rays, which are otherwise inaccessible.

Feasibility We simulated a GRB spectrum with flux 10^{-13} erg cm^{-2} s^{-1} using a photoelectric absorption plus power-law model and a 30 ks exposure (WebSpec). The simulation yields a reduced $\chi^2 \sim 0.9$ and a count rate of 0.01 cts/s, demonstrating that EPIC-MOS and EPIC-pn can achieve well-constrained spectral fits at these flux levels (Table 1). The fitted spectrum is shown in Figure 3.

Trigger Criteria Candidate bursts will be monitored with *Swift* XRT. A late-time spectral softening of $\Delta\beta \geq 1$, based on numerical simulations (Figure 1) and GRB 130907A (Figure 2), will trigger XMM observations.

Observation Plan We propose two XMM-Newton epochs, at 20 and 50 days post-burst, with 30 ks exposures each using EPIC-MOS and EPIC-pn in full-frame mode. XRT light curves will be extrapolated to ensure detectability. These observations will allow us to track spectral evolution and disentangle contributions from external-shock and dust-scattered emission.

Summary The proposed strategy ensures robust late-time spectral measurements, providing critical

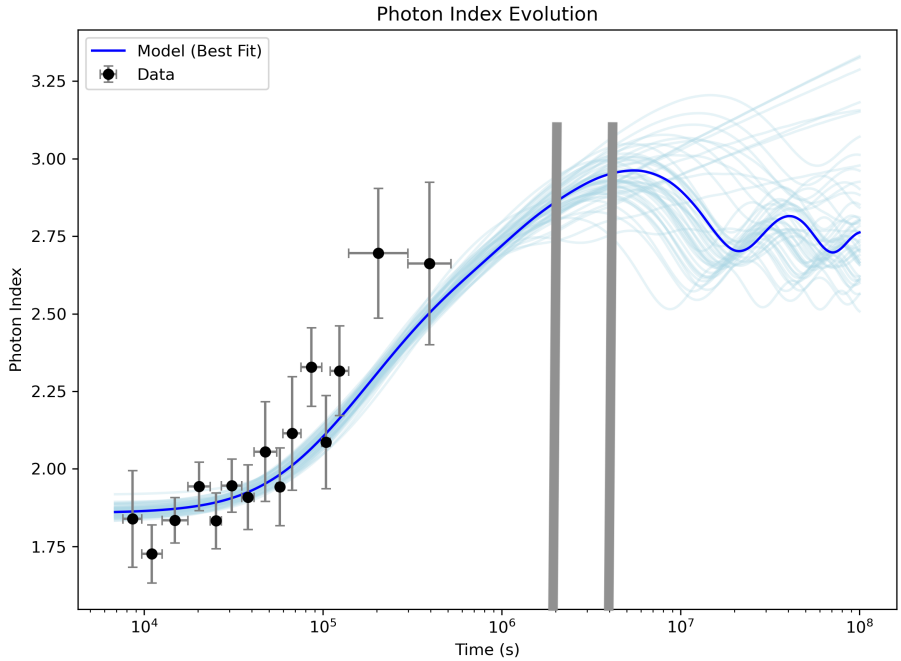

Figure 2: Spectral evolution of GRB 130907A, along with posterior predictive light curves from a model including both dust-reprocessed and external-shock emission (Mandayapuram et al., in preparation), is shown. The posterior distributions can be better constrained with late-time observations. For a future burst, we plan XMM-Newton observations at 20 and 50 days post-burst, indicated by the vertical grey lines.

constraints on GRB afterglow physics and dust scattering models.

par	comp	Model Compo-nent	Parameter	Unit	Value
1	1	zphabs	nH	10^{22}	0.94 ± 0.14
2	1	zphabs	Redshift	–	1.23800 (frozen)
3	2	zpowerlaw	PhoIndex	–	1.92 ± 0.05
4	2	zpowerlaw	Redshift	–	1.23800 (frozen)

Table 1: The best fit parameters with errors for the example spectrum. **Model:** zphabs* zpowerlaw.

4. Report on the last use of XMM-Newton data

We have not conducted XMM-Newton observations in past.

5. Most relevant proposer's publications

(1) Chakyar, S. P and **Resmi, L.** GRB jet parameters from raising optical afterglow light curves, ApJ, 2025, 983, 111. (2) Mondal, T.; Pramanick, S.; **Resmi, L.**; & Bose, D. Probing Gamma-Ray Burst afterglows with the Cherenkov Telescope Array, MNRAS, 2023, 522, 5690. (3) Misra, K; **Resmi, L**; Kann, D. A., et al., Low frequency view of GRB 1909114c reveals time varying shock microphysics, MNRAS, 2021, 504, 5685.MAGIC Collaboration; Acciari, V. A.; Ansoldi, S.; (including **Resmi L.**), Observation of inverse Compton emission from a long gamma-ray burst, Nature, 2019, 575, 459. (4) Lamb, Gavin P.; Mandel, Ilya; **Resmi, Lekshmi.**, Late-time evolution of afterglows from off-axis neutron star mergers, MNRAS, 2018, 481, 2581. (5) **Resmi, L.**; Schulze, S.; Ishwara-Chandra, C. H.; Misra, K.; Buchner, J.; De Pasquale, M.; Sánchez-Ramírez, R.; Klose, S.; Kim, S.; Tanvir, N. R.; O'Brien, P. T., Low-frequency View of GW170817/GRB 170817A with the Giant Metrewave Radio Telescope, ApJ, 2018, 867, 57. (6) Saleem, M.; **Resmi, L.**; Misra, Kuntal; Pai, Archana; Arun, K. G., Exploring short-GRB afterglow parameter space for observations in coincidence with gravitational waves, MNRAS, 2018, 474, 5340. (7) Kim, S.; Schulze, S.; **Resmi, L.**, ALMA and GMRT Constraints on the Off-axis Gamma- Ray Burst 170817A from the Binary Neutron Star Merger GW170817, ApJ Letters, 2017, 850, 21.

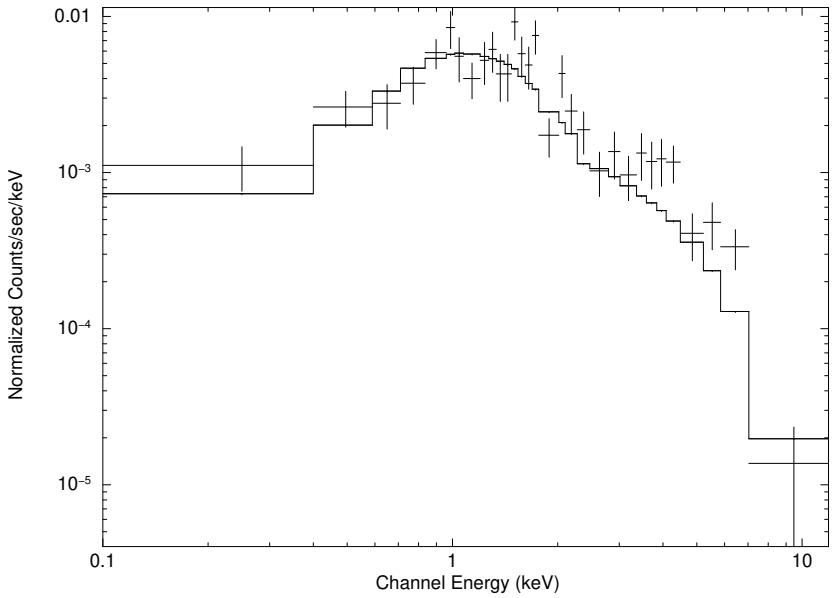

Figure 3: Simulation of GRB130907 spectrum using WebSpec

Bibliography

1. Crowther, P.A. 2003, Astrophysics and Space Science 285, 677.
2. Evans, P. A. et al. 2014, MNRAS, 444, 250.
3. Galama, T. J. et al. 1998, Nature, 395, 670.
4. Hjorth, J. et al. 2003, Nature, 423, 847.
5. Holland, S. T. et al. 2010, ApJ, 717, 223.
6. Irwin, C. M. & Chevalier, R. 2016, MNRAS, 460, 1680.
7. Klose, S. 1998, ApJ, 507, 300.
8. Margutti, R. et al. 2015, ApJ, 805, 159.
9. Mészáros et al. 2000, ApJ,5431, L35.
10. Miralda-Escudé, J. 1999, ApJ, 512, 21.
11. Perley, D. A. et al. 2013, ApJ, 778, 128.
12. Schady, P. et al. 2012, A&A, 537, 15.
13. Shao, L. & Dai, Z. G. 2007, ApJ, 660, 1319.
14. Shao, L. et al. 2008, ApJ, 675, 507.
15. Shen, R.-F. et al. 2009, MNRAS, 393, 598.
16. Tuthill, P. G. et al.1999, Nature, 398, 487.
17. Wang et al. 2016, ApJ, 818, 167.